Electronic Supplementary Material (ESI) for Energy & Environmental Science.

Supplementary information

Sodium Intercalation Chemistry in Graphite

Haegyeom Kim[a†], Jihyun Hong[a†], Gabin Yoon[a, b†], Hyunchul Kim[c], Kyu-Young Park[a], Min-Sik Park[d], Won-Sub Yoon[c], and Kisuk Kang[a,b*]

a. Department of Materials Science and Engineering, Research Institute of Advanced Materials (RIAM), Seoul National University, Gwanak-ro 599, Gwanak-gu, Seoul 151-742, Republic of Korea

b. Center for nanoparticle research, Institute for Basic Science (IBS), Seoul National University, Gwanak-ro 599, Gwanak-gu, Seoul 151-742, Republic of Korea

c. Department of Energy Science, Sungkyunkwan University, Suwon 440-746, Republic of Korea

d. Advanced Batteries Research Center, Korea Electronics Technology Institute, Seongnam 463-816, Republic of Korea

† These authors are equally contributed to this work.

Corresponding Author

Kisuk Kang, E-mail address: matlgen1@snu.ac.kr

Tel.: +82-2-880-7088 Fax.: +82-2-885-9671

Contents

1. Experimental and computational details

Materials

Natural graphite was purchased from Bay Carbon Inc. and used without any modification or post-treatment. The electrolytes were carefully prepared to maintain low H_2O contents (<20 ppm). The Na salt ($NaPF_6$) and molecular sieves were stored in a vacuum oven at 180°C before use. The dried Na salts were dissolved in electrolyte solvents, including diethylene glycol dimethyl ether (DEGDME), tetraethylene glycol dimethyl ether (TEGDME), and dimethoxyethane (DME) at 1 M. The solutions were stirred at 80°C for 2 days, and molecular sieves were used to remove residual H_2O from the electrolyte solutions.

Electrode preparation and electrochemical measurements

Graphite electrodes were prepared by mixing the active material (natural graphite, 90 wt%) with polyvinylidene fluoride binder (PVDF, 10 wt%) in an N-methyl-2-pyrrolidone (NMP) solvent. The resulting slurry was uniformly pasted onto Cu foil, dried at 120°C for 1 h, and roll-pressed. The average electrode thickness was ~40 μm. Test cells were assembled in a glove box into a two-electrode configuration with a Na metal counter electrode. A separator of grade GF/F (Whatman, USA) was sonicated in acetone and dried at 120°C before use. Electrochemical profiles were obtained over a voltage range of 2.5 to 0.001 V using a multichannel potentio-galvanostat (WonATech).

In operando XRD analysis

For in operando XRD analysis, the holed coin cells, which were sealed by kapton film with epoxy, were used. In operando XRD patterns for graphite were collected on the 5A XRD beamline at PLS-II. The wavelength of the X-ray beam was 0.7653 Å, and XRD patterns were recorded as a set of circles on a Mar 345-image plate detector in the transmission mode for approximately 1 min of exposure time. The storage ring was operated with an electron energy of 3.0 GeV and a current of 300 mA. The total recording time was approximately 2.6 min because of the scanning time of the image plate and transferring time of the spectral information. The two theta angles of all the XRD patterns presented in this article have been recalculated to corresponding angles for λ = 1.54 Å, which is the wavelength of the conventional X-ray tube source with Cu Kα radiation for ease of comparison with other published results.

Calculation details

Geometric optimizations of [Na-ether]$^+$ complexes were conducted with the DFT platform using Gaussian 09 program.[1] All the molecular structures were fully relaxed with the B3LYP/6-311G level. Structural relaxations of stage 1 and stage 2 GICs were performed with the Vienna ab initio simulation package (VASP).[2] We used a projector-augmented wave (PAW) pseudopotential[3], as implemented in VASP, and the exchange-correlation energy was addressed using the Perdew-Burke-Ernzerhof (PBE) parameterized generalized gradient approximation (GGA).[4] In addition, the semi-empirical dispersion potential (DFT-D2)[5] was implemented to describe the van der Waals (vdW) interactions of graphite. All the GIC structures were relaxed until the total energy of the system converged within 0.01 eV/Å.

2. Solvation structure of [Na-DEGDME]$^{+}$ complex

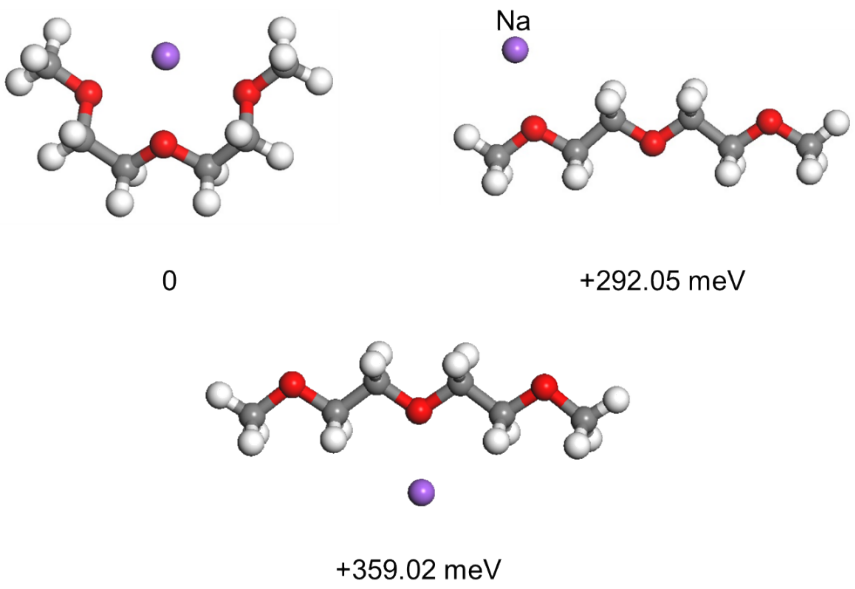

Figure S1. Various configurations of [Na-DEGDME]$^{+}$ solvation complex. Energies relative to the most stable configuration are shown with each structure.

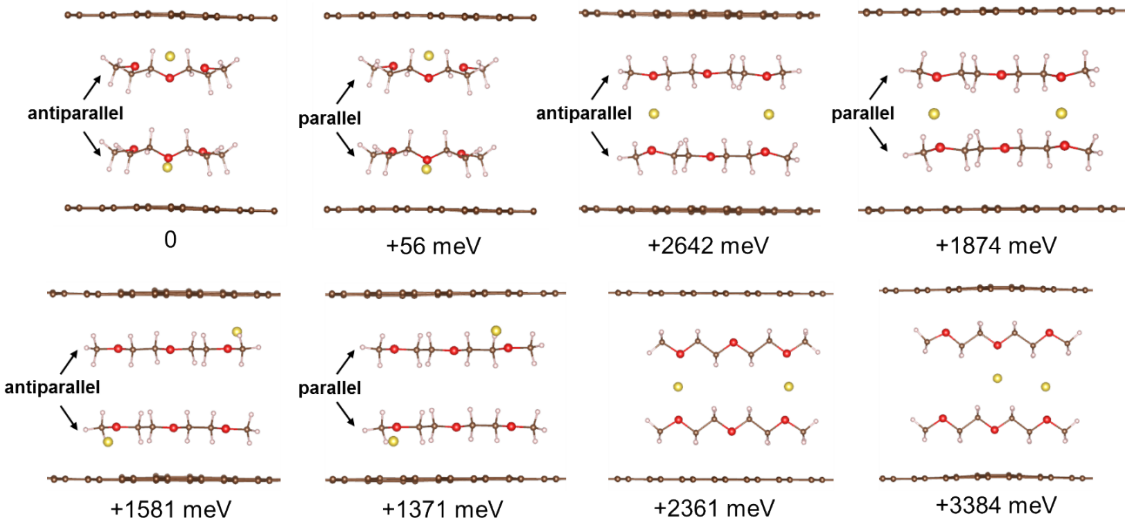

Figure S2. Various configurations of double complex intercalation of $[Na\text{-}DEGDME]^+$ in stage 1 structure.

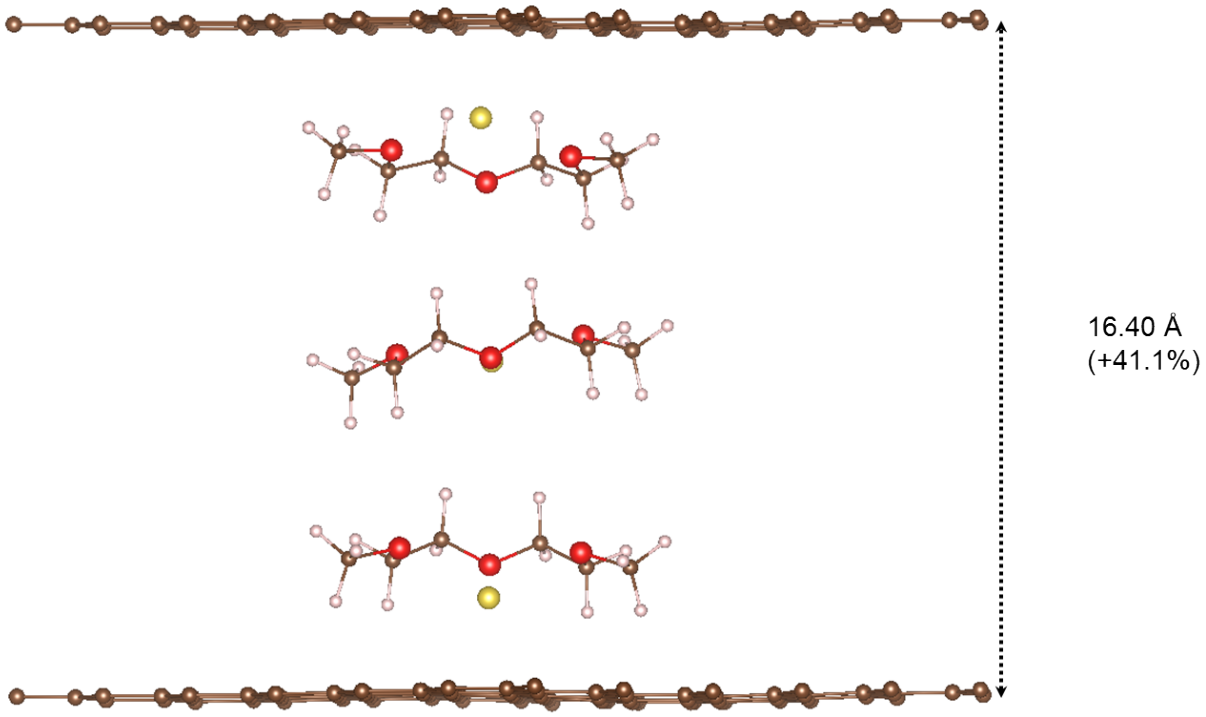

Figure S3. A model of triple complex intercalation of $[Na\text{-}DEGDME]^+$ in stage 1 structure.

3. Calculation of maximum density of [Na-DEGDME]$^+$ complex in graphene interlayer gallery

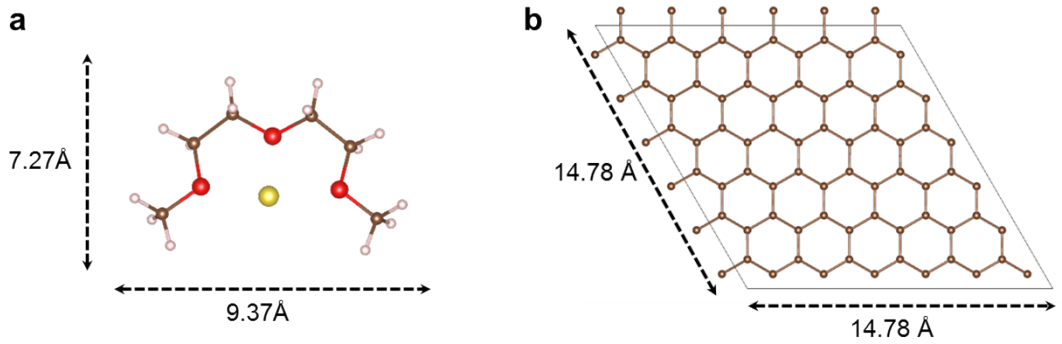

Figure S4. Calculated planar area of **a.** [Na-DEGDME]$^+$ and **b.** graphene layer. For convenience, rectangular shape of [Na-DEGDME]$^+$ is assumed and intermolecular interactions are considered in Figure S4a. The planar areas of [Na-DEGDME]$^+$ and graphene layer are 68.13 Å^2 per complex, and 2.64 Å^2 per carbon atom, respectively.

4. Charge density in graphene layers upon sodium intercalation

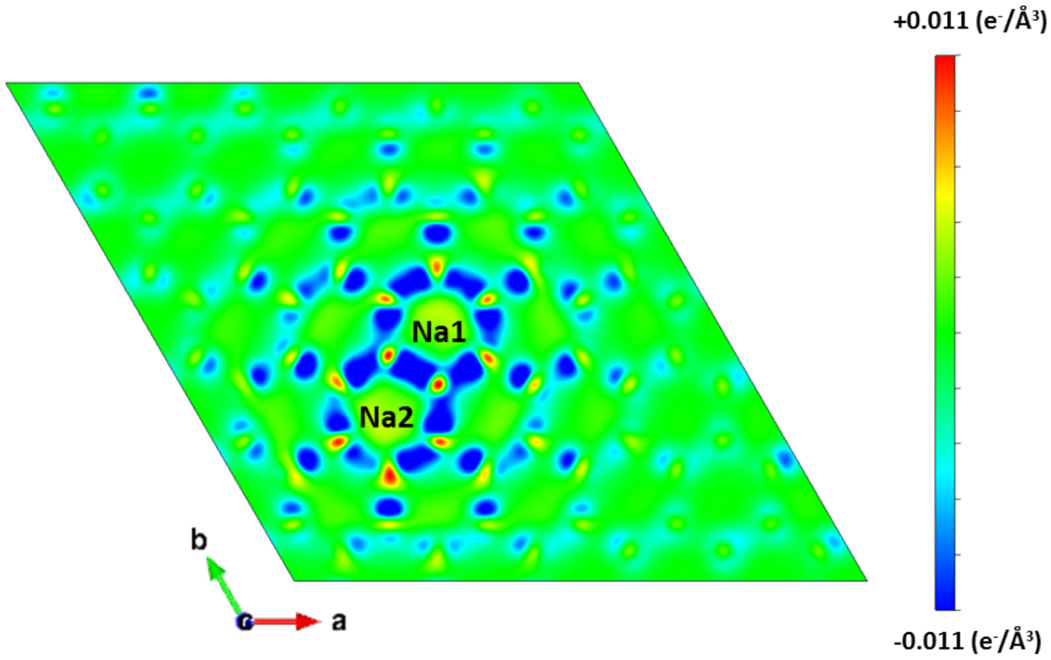

Figure S5. In-plane charge distribution at graphene layer after the intercalation of [Na-DEGDME]$^{+}$ complex. Intercalated Na^{+} ions donate electrons to graphene layer, forming an ionic bond with electrons from C-C bonds in graphene layer.

5. Solvated-Na intercalation mechanism with three solvent species

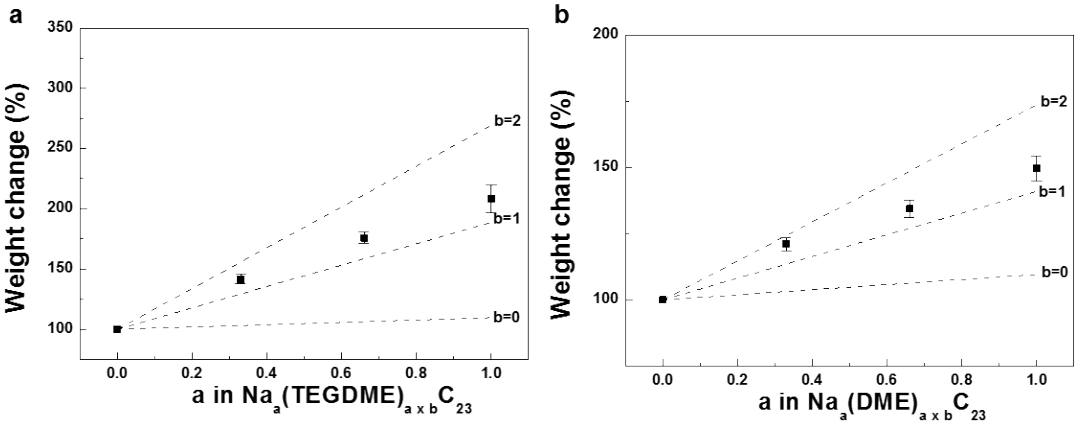

Figure S6. Mass change of the electrodes upon discharge when **a.** TEGDME and **b.** DME solvents are used.

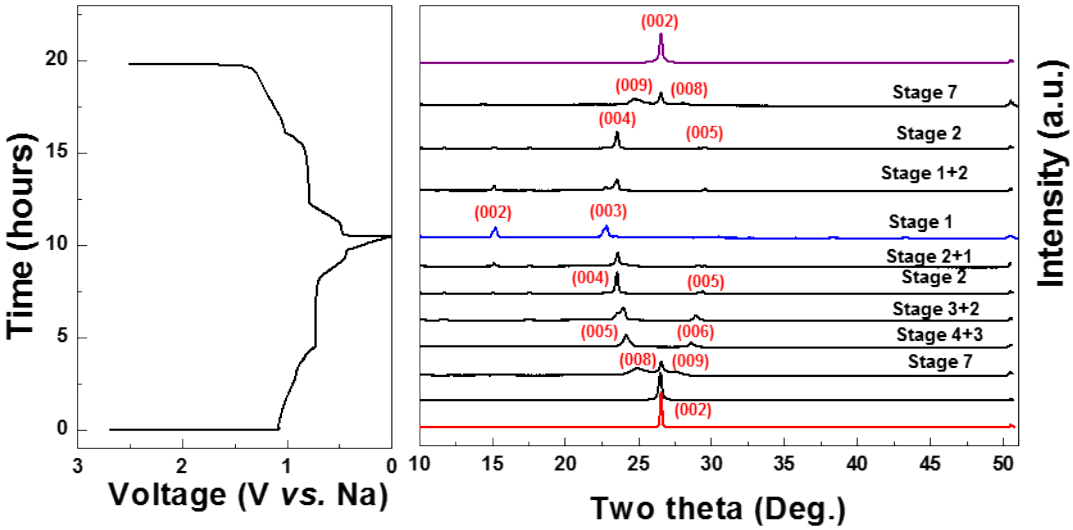

Figure S7. Typical charge/discharge profile and ex-situ XRD patterns using 1M $NaPF_6$ in TEGDME electrolyte.

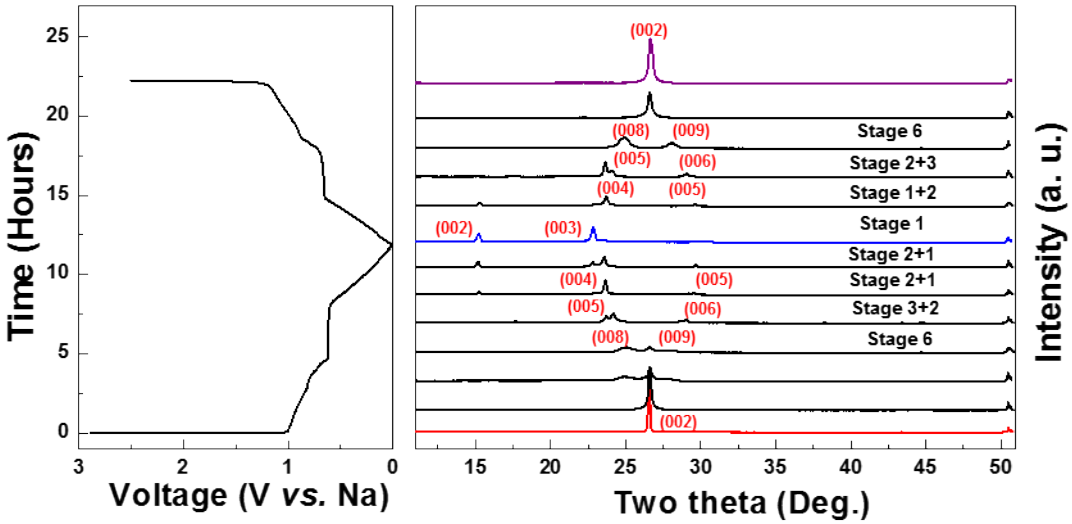

Figure S8. Typical charge/discharge profile and ex-situ XRD patterns using 1M $NaPF_6$ in DEGDME electrolyte.

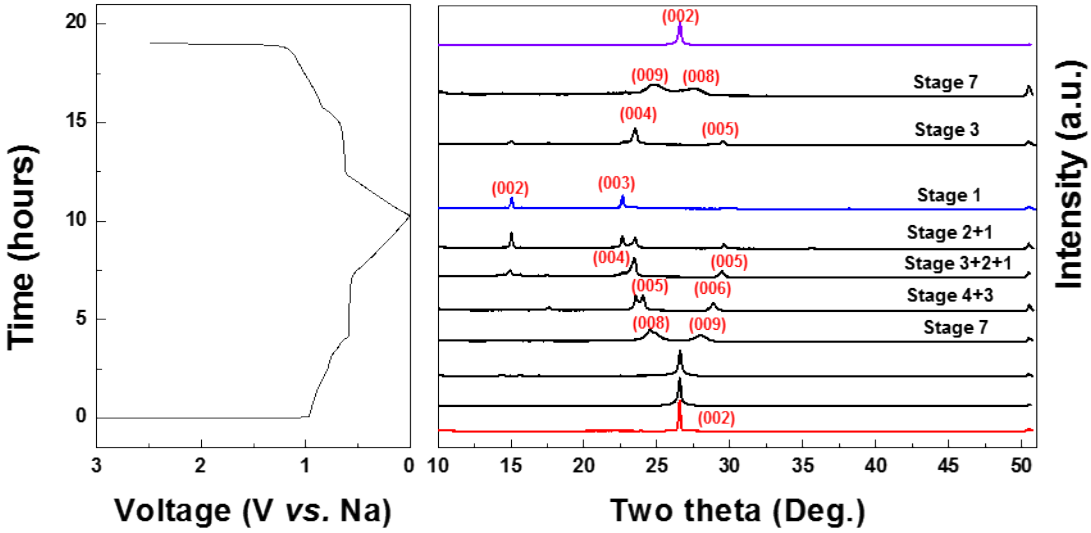

Figure S9. Typical charge/discharge profile and ex-situ XRD patterns using 1M $NaPF_6$ in DME electrolyte.

6. Ordering of [Na-DEGDME]$^{+}$ complexes in the model structure

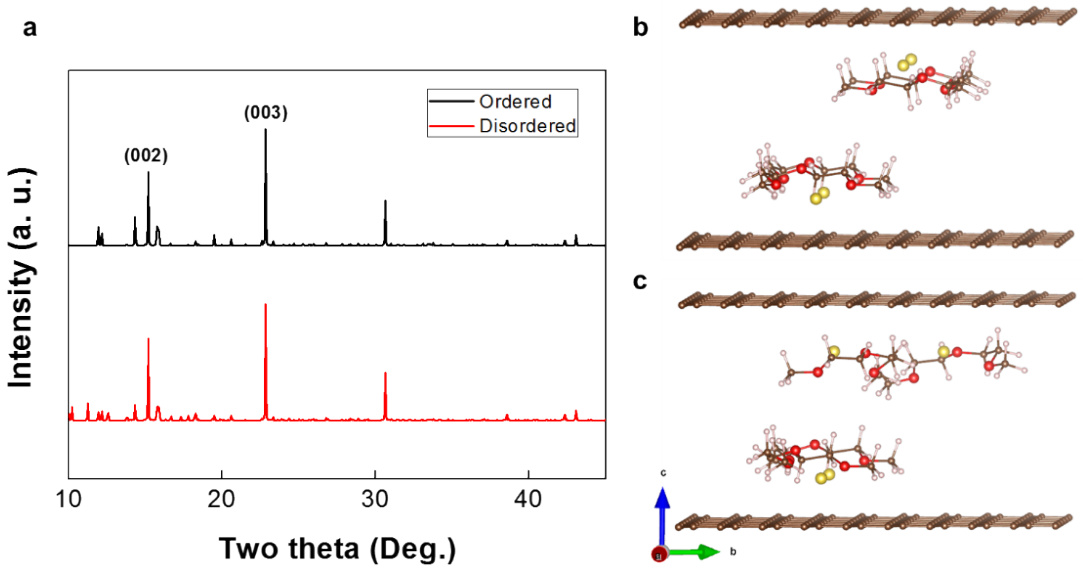

Figure S10. a. Simulated XRD patterns of two different state of [Na-DEGDME]$^{+}$ ordering in graphite host. Structures of ordered, disordered structures used in simulation are described in **b.**, **c.**, respectively. Note that the intensity ratio of (002) / (003) does not change, whereas several minor peaks in 11˚-22˚ range emerge or diminish due to the change of [Na-DEGDME]$^{+}$ ordering.

7. Cycle performance of graphite electrode

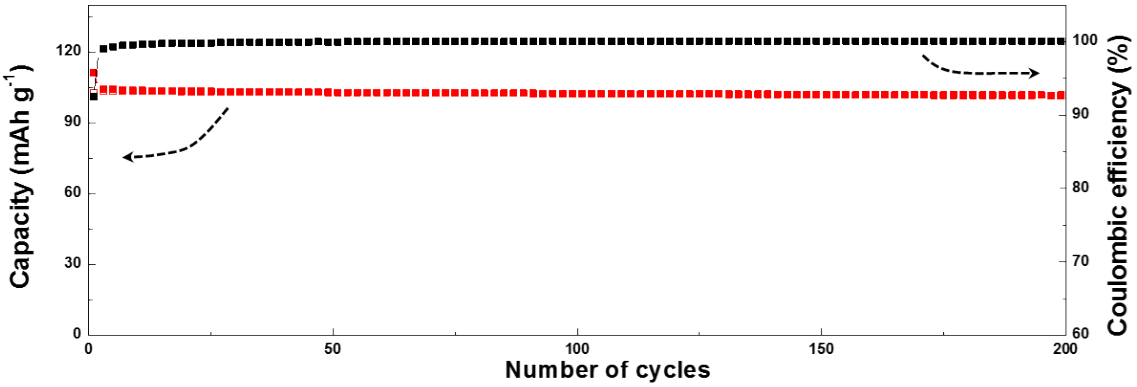

Figure S11. Cycle stability of graphite electrode in Na half cells. Graphite working electrode, Na metal counter electrode, and 1M $NaPF_6$ in DEGDME electrolyte are used.

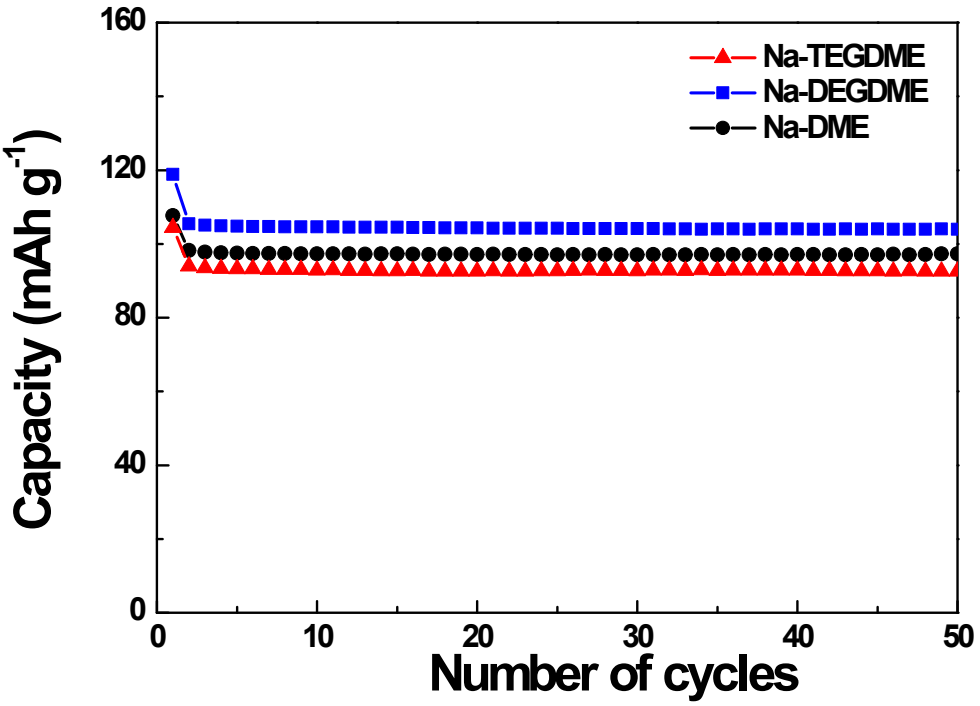

Figure S12. Cycle stability of graphite electrode in Na half cells. Graphite working electrode, Na metal counter electrode are used. 1M $NaPF_6$ in TEGDME, DEGDME, DME electrolytes are used, respectively.

8. Stability of graphite electrode after cycling

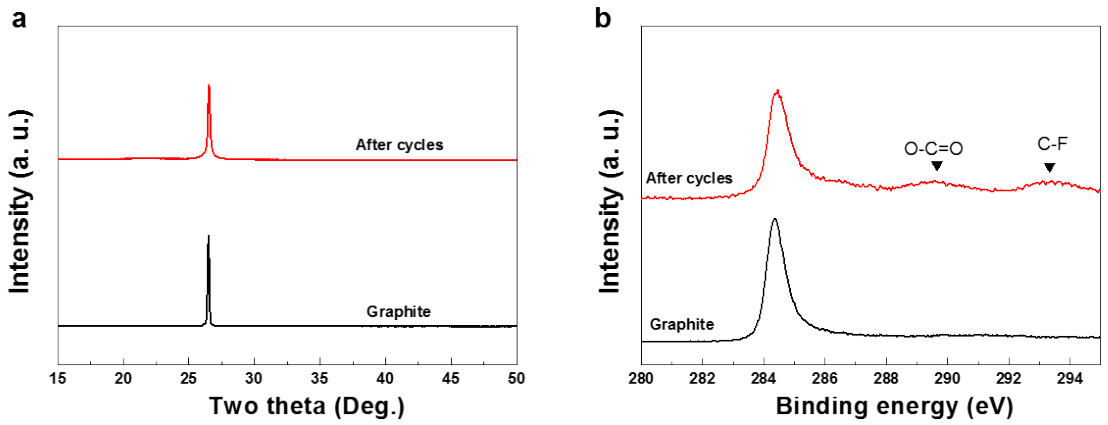

Figure S13. Ex-situ XRD and XPS analyses before and after cycling. a. XRD patterns of graphite electrode before/after cycling. **b.** XPS spectra of graphite electrode before/after cycling.

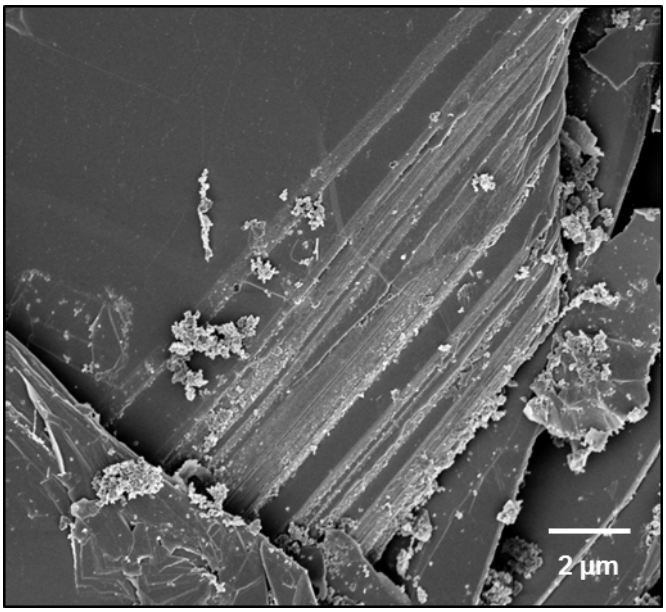

Figure S14. SEM image of graphite electrode after cycling.

References

1. M. J. Frisch, G. W. Trucks, H. B. Schlegel, G. E. Scuseria, M. A. Robb, J. R. Cheeseman, G. Scalmani, V. Barone, B. Mennucci, G. A. Petersson, H. Nakatsuji, M. Caricato, X. Li, H. P. Hratchian, A. F. Izmaylov, J. Bloino, G. Zheng, J. L. Sonnenberg, M. Hada, M. Ehara, K. Toyota, R. Fukuda, J. Hasegawa, M. Ishida, T. Nakajima, Y. Honda, O. Kitao, H. Nakai, T. Vreven, J. A. Montgomery Jr., J. E. Peralta, F. Ogliaro, M. J. Bearpark, J. Heyd, E. N. Brothers, K. N. Kudin, V. N. Staroverov, R. Kobayashi, J. Normand, K. Raghavachari, A. P. Rendell, J. C. Burant, S. S. Iyengar, J. Tomasi, M. Cossi, N. Rega, N. J. Millam, M. Klene, J. E. Knox, J. B. Cross, V. Bakken, C. Adamo, J. Jaramillo, R. Gomperts, R. E. Stratmann, O. Yazyev, A. J. Austin, R. Cammi, C. Pomelli, J. W. Ochterski, R. L. Martin, K. Morokuma, V. G. Zakrzewski, G. A. Voth, P. Salvador, J. J. Dannenberg, S. Dapprich, A. D. Daniels, Ö. Farkas, J. B. Foresman, J. V. Ortiz, J. Cioslowski and D. J. Fox, Gaussian, Inc., Wallingford, CT, USA, 2009.

2. G. Kresse and J. Furthmüller, *Comp. Mater. Sci.*, 1996, **6**, 15-50.

3. P. E. Blöchl, *Phys. Rev. B*, 1994, **50**, 17953-17979.

4. J. P. Perdew, K. Burke and M. Ernzerhof, *Phys. Rev. Lett.*, 1996, **77**, 3865-3868.

5. S. Grimme, *J. Comput. Chem.*, 2006, **27**, 1787-1799.